PREPARATION AND PROPERTIES OF NANOCOMPOSITES PREPARED FROM SHORTENED, FUNCTIONALIZED SINGLE-WALLED CARBON NANOTUBES

J. G. Smith Jr.[1], D. M. Delozier[2], K. A. Watson[2],
J. W. Connell[1], Aiping Yu[3], R. C. Haddon[3] and E. Bekyarova[3]

[1]NASA Langley Research Center, Hampton, VA 23681-2199;
[2]National Institute of Aerospace Research, 100 Exploration Way, Hampton, VA 23666-6147;
[3]University of California, Riverside, Department of Chemistry, Riverside, CA 92521

ABSTRACT

As part of a continuing materials development activity, low color space environmentally stable polymeric materials that possess sufficient electrical conductivity for electrostatic charge dissipation (ESD) have been investigated. One method of incorporating sufficient electrical conductivity for ESD without detrimental effects on other polymer properties of interest (i.e., optical and thermo-optical) is through the incorporation of single-walled carbon nanotubes (SWNTs). However, SWNTs are difficult to fully disperse in the polymer matrix. One means of improving dispersion is by shortening and functionalizing SWNTs. While this improves dispersion, other properties (i.e., electrical) of the SWNTs can be affected which can in turn alter the final nanocomposite properties. Additionally, functionalization of the polymer matrix can also influence nanocomposite properties obtained from shortened, functionalized SWNTs. The preparation and characterization of nanocomposites fabricated from a polyimide, both functionalized and unfunctionalized, and shortened, functionalized SWNTs will be presented.

KEY WORDS: Carbon Nanotubes, High Temperature Polymers, Polyimides, ESD Films

1. INTRODUCTION

An enabling technology in the development of Gossamer spacecraft is space environmentally durable polymeric materials (i.e., films, coating, moldings, etc.). These are large, deployable, ultra lightweight vehicles that are stowed in a compact container on a conventional launch vehicle prior to launch. This requires the film-based components to be fairly compliant so as to be folded into a compact volume. Once orbit is achieved, the vehicle automatically deploys to its full size which can be many square meters (1). Two "proof-of-concept" examples are the Znamya-2 launched in 1993 and the inflatable antennae experiment (IAE) deployed from the space shuttle Endeavor (STS-77) in 1996. These vehicles used Mylar® or its equivalent in the demonstrations. Since the flight tests were demonstrations of the concept, the environmental stability of the polymer was not a concern.

Future Gossamer spacecraft will also require that film-based materials be durable to the space environment. Depending on the orbital location of the vehicle, the film must exhibit resistance to environmental hazards such as atomic oxygen in low Earth orbit, UV and vacuum UV radiation, electrons/ions, solar flare protons and galactic cosmic rays (2-4). Energetic charged particles (e.g. electrons) are also present which can penetrate the material surface and deposit a charge onto an insulating polymer. Over time this electrostatic charge (ESC) can accumulate and be dissipated (electrostatic charge dissipation, ESD) in a single event on surrounding surfaces (i.e., films, electronics, etc.) causing considerable damage. The surface resistivity needed to dissipate ESC is in the range of 10^6 to 10^{10} Ω/square.

Many of the physical properties, with the exception of electrical conductivity, needed for Gossamer materials can be met using aromatic polyimides by the appropriate choice of constituent monomers (5,6). Conductive and transparent coatings such as indium tin oxide have been used on spacecraft; however, these are typically brittle and would lose their conductive attributes if folded. Previous work has identified single-walled carbon nanotubes (SWNTs) as a practical solution due to their nanometer size and exceptional properties. This is important since some mission applications require films with low solar absorptivity (synonymous with low color), optical transparency, and high thermal emissivity as well as conductivity. SWNTs have afforded the electrical resistivites needed for ESD with minimal affect on the optical and thermo-optical (solar absorptivity and thermal emissivity) properties. This has been attained in bulk loading in the polymer (7-9) and as a surface layer (e.g. Bucky paper) via SWNT spray coating (10-14). Bulk loading provides conductivity through the thickness whereas SWNT spray coating provides only a single conductive surface.

SWNTs have been prepared by processes such as high-pressure carbon monoxide (HiPco), electric arc (EA), laser ablation, and chemical vapor deposition (15, 16). It is known that improvements in certain mechanical and physical properties of a host polymer as compared to

the virgin material can be obtained by incorporating nanomaterials provided, that the nanomaterials are uniformly dispersed throughout the matrix. However, this has been difficult to achieve with SWNTs due to their insolubility and/or incompatibility with the host resin. Typically, SWNTs tend to agglomerate as bundles both in solvents and the host resin. Once dispersed, the SWNTs reagglomerate soon thereafter due to van der Waals forces. One method of improving SWNT dispersability and solubility is through shortening the tubes. Treatment of SWNTs with nitric or nitric/sulfuric acids is known to shorten the tubes and also introduce carboxylic acid functionalities at the tube ends (17, 18). Shortening the SWNTs too much though can negatively affect the properties (e.g. electrical).

The current work evaluated SWNTs prepared by the EA method and compared the resulting nanocomposite properties with those obtained using HiPco SWNTs. A single HiPco SWNT exhibits a large aspect ratio due to its relatively small diameter (19), but the tubes are often present in bundles making the effective aspect ratio smaller. A single EA SWNT is known to have a larger diameter than the HiPco material and thus a smaller aspect ratio by comparison (20). Consequently, it was of interest to determine if the aspect ratio was a major factor in achieving the necessary conductivity in the nanocomposite. The EA-SWNTs were obtained as functionalized and as carboxylic acid functionalized materials. These were incorporated in an alkoxysilane terminated amide acid oligomer of LaRC™ CP2 that was subsequently thermally converted to the corresponding imide. Alkoxysilanes are known to aid in the adhesion of organic materials to inorganic substrates through the formation of an oxane bond. This bond is thermally generated from the condensation of silanol groups present on the organic substrate, typically under acidic or basic hydrolysis conditions, with functionalities (typically hydroxyl or carboxylic) present on the inorganic component. Hydroxyl functionalities present on the inorganic may be naturally occurring or generated through chemical reactions on the inorganic surface. In this case, the alkoxysilane groups, once hydrolyzed, could react with the carboxylic acid groups present on the modified SWNTs (8). The preparation of LaRC™ CP2 nanocomposites prepared via an *in-situ* method using the carboxylic acid functionalized EA-SWNTs has recently been reported (21). It was found that good dispersion was achieved in the matrix. However, to attain the electrical resistivities necessary for ESD a high loading level was required which negatively impacted the optical properties. Due to the solubility of LaRC™ CP2 in the imide form, the acid functionalized EA-SWNTs were incorporated into the matrix to assess the effect of matrix functionality upon the optical and electrical properties. The preparation and characterization of nanocomposites prepared from the two forms of EA-SWNTs in LaRC™ CP2 materials are described herein.

2. EXPERIMENTAL

2.1 Starting Materials The following chemicals were obtained from the indicated sources and used without further purification: aminophenyltrimethoxysilane (APTS, Gelest Inc., 90% meta, 10% para), 1,3-bis(3-aminophenoxy)benzene [APB, Mitsui Chemicals America, Inc., melting point (m.p.) 107-108.5°C], and N,N-dimethylacetamide (DMAc, Aldrich). 4,4'-Hexafluoroisopropylidene diphthalic anhydride (6-FDA, Hoechst Celanese Inc., m.p. 241-243 °C) was sublimed prior to use. All other chemicals were used as received without further purification. LaRC™ CP2 polyimide powder was obtained from SRS Technologies, Inc. (6). SWNTs, synthesized by the electric arc method (EA-SWNT) using Ni and Y as a catalyst mixture in the ratio of 4:1 (22, 23) were obtained from Carbon Solutions, Inc. (www.carbonsolution.com) and purified by air oxidation followed by treatment in aqueous HCl to remove metal residue. The EA-SWNTs were treated with nitric acid treatment to incorporate carboxylic functionality and defined as nitric acid treated SWNTs (NAT-SWNTs) (17, 18).

2.2 Synthesis of Alkoxysilane Terminated Amide Acid Oligomer An alkoxysilane terminated amide acid (ASTAA) of LaRC™ CP-2 was prepared by the reaction of 6-FDA with APB and end-capped with APTS at a 2.5% offset. A representative procedure is described. To a 100 mL round bottom flask equipped with a nitrogen inlet, mechanical stirrer, and drying tube filled with calcium sulfate was charged APB (9.0703 g, 0.0310 mol) and APTS (0.3394 g, 0.0016 mol). These were dissolved in DMAc (10 mL) at room temperature under nitrogen. The flask was subsequently immersed in a water bath to dissipate the heat of reaction due to the dianhydride addition. 6-FDA (14.1368 g, 0.0318 mol) was added in one portion as a slurry in DMAc (17 mL) to the solution and rinsed in with 20 mL of DMAc to afford a solution with a solids content of ~35%. The reaction mixture was stirred for ~24 h at room temperature under nitrogen. The inherent viscosity (η_{inh}) was 0.66 dL/g in DMAc at 25°C. The solution was used as is or SWNTs were added as described in 2.3 and 2.4.

2.3 Blending of SWNTs and ASTAA Nanocomposite solutions were prepared by the addition of a sonicated mixture of SWNTs (EA-SWNTs or NAT-SWNTs) in DMAc to a pre-weighed polymer solution while stirring. The loadings of SWNTs were determined in weight (wt) % based on the mass of polymer used. A representative procedure is described. To a 100 mL round bottom flask equipped with nitrogen inlet, mechanical stirrer, and drying tube filled with calcium sulfate was charged 5.75 g of an ASTAA solution (~35% solids). In a separate tared vial, EA-SWNTs (0.0062 g) were placed in 3 mL of DMAc and the mixture sonicated for ~2.5 h in a Degussa-Ney ULTRAsonik 57X Cleaner operated at ~50% power and degas levels. The initial temperature of the water bath was ambient and ~40°C at the conclusion of sonication. The suspended tubes were subsequently added to the stirred mixture of ASTAA at room temperature and rinsed in with 1.2 mL of DMAc to afford a solids content of ~20%. The SWNT

loading was ~0.3 wt %. The mixture was stirred under a nitrogen atmosphere at room temperature for ~16 h prior to film casting.

2.4 NAT-SWNTs in LaRC™ CP2 Nanocomposite solutions were prepared by the addition of a sonicated mixture of SWNTs in DMAc to a known quantity of LaRC™ CP2 dissolved in DMAc. A representative procedure is described. To a 100 mL round bottom flask was charged 3.03 g of polyimide powder. The flask was then fitted with a nitrogen inlet, mechanical stirrer, and drying tube filled with calcium sulfate and charged with 6 mL of DMAc to afford a ~35% solids content. In a separate tared vial, NAT-SWNTs (0.0031 g) were placed in 3 mL of DMAc and the mixture sonicated for ~2.5 h as described in 2.3. The suspended tubes were subsequently added to the stirred mixture and rinsed in with 4 mL of DMAc to afford a solids content of ~20%. The SWNT loading was ~0.1 wt %. The mixture was stirred under a nitrogen atmosphere at room temperature for ~16 h prior to film casting.

2.5 Films DMAc solutions of 2.2 - 2.4 were doctored onto plate glass and dried to tack free forms in a low humidity chamber at ambient temperature. The films were cured on the glass plate in a forced air oven at 100, 200, and 300°C for 1 h each. The films were subsequently removed from the glass plate and characterized. Room temperature thin-film tensile properties were determined according to ASTM D882 using four specimens.

2.6 Characterization Inherent viscosities (η_{inh}) were obtained on 0.5% (w/v) amide acid solutions in DMAc at 25°C. Differential scanning calorimetry (DSC) was conducted on a Shimadzu DSC-50 thermal analyzer. Melting point ranges (tangent of onset to melt and the endothermic peak) were determined at a heating rate of 10°C/min. Glass transition temperatures (T_gs) were determined at a heating rate of 20 °C/min and taken as the inflection point of the ΔH vs. temperature curve. FTIR was obtained on a Nicolet Magna-IR 560 ESP spectrometer on KBr pellets. Raman spectroscopy was performed using a Thermo Nicolet Almega Dispersive Raman spectrometer equipped with a 785 nm laser. UV/VIS spectra were obtained on thin films using a Perkin-Elmer Lambda 900 UV/VIS/NIR and Shimadzu UV3100 UVVIS/NIR spectrometers. Near-IR (NIR) spectra were obtained on dimethylformamide solutions at a SWNT concentration of 0.01 mg/mL on a Varian Cary 500 spectrophotometer. Atomic force microscopy (AFM) images were obtained on a Digital Instruments Nanoscope IIIA operating in the taping mode. Solar absorptivities (α) were measured on an AZ Technology Model LPSR-300 spectroreflectometer with measurements taken from 250 to 2800 nm with a vapor deposited aluminum on Kapton® film (1st surface mirror) as a reflective reference for air mass 0 per ASTM E903. An AZ Technology Temp 2000A infrared reflectometer was used to measure thermal emissivity (ε). High-resolution scanning electron microscopy (HRSEM) images were obtained on Hitachi S-4700 and S-5200 field emission scanning electron microscopy systems. Surface resistance was determined per EOS/ESD Standard S-11.11-1993 using a Prostat® PRS-801 Resistance System operating at 10 - 100 volts and reported as an average of three readings.

Volume resistivity was determined using a Prostat® PRS-801 Resistance System with a PRF-911 Concentric Ring Fixture operating at 10 - 100 volts according to ASTM D-257.

3. RESULTS AND DISCUSSION

The overall objective of this work was to develop low color, optically transparent, space environmentally durable polymer nanocomposites with sufficient conductivity to dissipate static charge build-up. Prior work using SWNTs prepared by the HiPco process exhibited good performance in bulk loading (7-9) and spray coating (10-14) of LaRC™ CP2 based materials. Based on the different aspect ratio afforded by the EA-SWNTs, it was of interest to evaluate this with respect to the optical and electrical properties of LaRC™ CP2 nanocomposites.

3.1 SWNTs The work presented herein assessed SWNTs prepared by the electric arc (EA) method vs. the HiPco process and their subsequent functionalization with carboxylic acid moieties using a nitric acid treatment. The as-prepared EA-SWNTs were purified by air oxidation followed by treatment in HCl to remove residual metal catalyst. Typically this purification procedure provided SWNTs with little or no functionality. The relative purity of SWNTs was estimated from the spectral region of the second interband transition for semiconducting SWNTs (S_{22}, spectral cutoff 7750 cm^{-1}–11750 cm^{-1}) in the NIR spectra against reference material R2 (20). Based on this method the relative carbonaceous purity of EA-SWNTs was ~80% (Figure 1). The Raman spectrum showed the expected absorption peaks associated with SWNTs. By AFM, the EA-SWNTs have an average diameter and length of 4–6 nm and 1 μm, respectively. In comparison, HiPco SWNTs had a relative carbonaceous purity of 88% and an average diameter and length of ~1 nm and 1-2 μm, respectively.

The EA-SWNTs were treated with nitric acid (NAT-SWNTs), which is known to introduce carboxylic acids onto the open ends and defect sites on SWNTs (17, 20). The formation of these

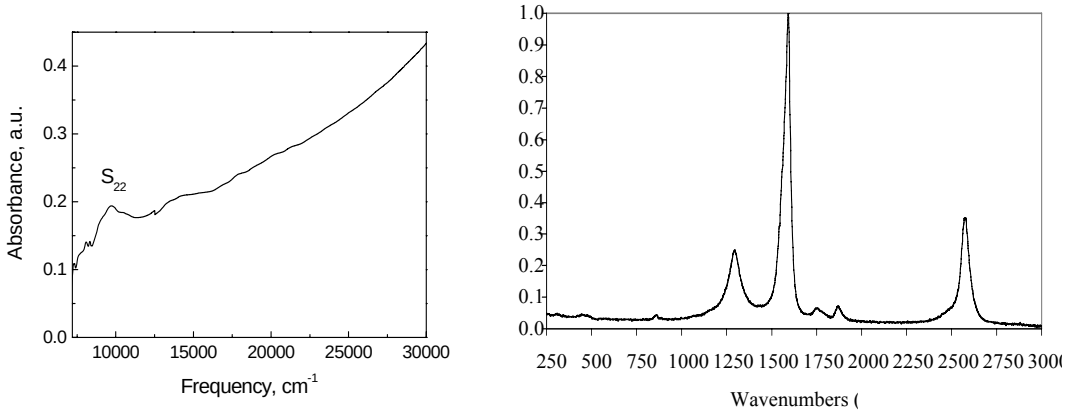

a b

Figure 1. Solution phase a) NIR and b) Raman spectra of EA-SWNTs.

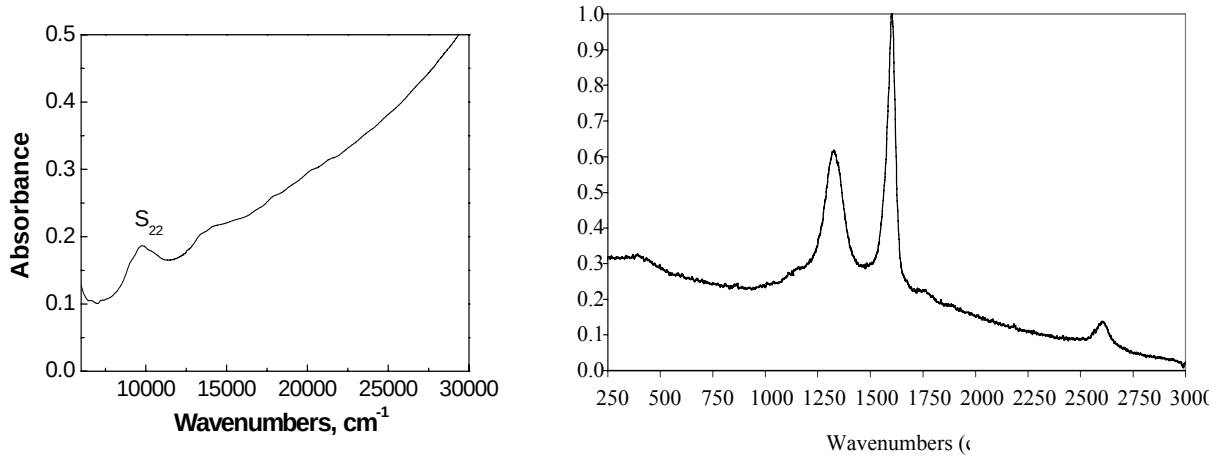

a b

Figure 2. Solution phase a) NIR and b) Raman spectra of NAT-SWNTs

groups was confirmed by a carbonyl stretching band at 1730 cm^{-1} in the infrared spectrum. The relative carbonaceous purity as determined from the solution phase NIR spectrum was ~95% (Figure 2). The Raman spectra showed a greater percentage of the carbon was sp^3-hybridized compared to the unfunctionalized EA-SWNTs. By AFM, the NAT-SWNTs consisted of bundles with an average diameter and length of 3-5 nm and ~0.8 μm, respectively. These tubes were slightly shorter than the unfunctionalized EA-SWNTs as a result of the nitric acid treatment.

3.2 Nanocomposites Prepared from Alkoxysilane Terminated LaRC™ CP2 Amide Acids

The approach taken to homogeneously disperse the SWNTs involved the use of oligomeric materials terminated with reactive endgroups (i.e., trimethoxy silane). Based on the LaRC™ CP2 backbone, oligomers were prepared at a stoichiometric offset of 2.5% corresponding to a calculated $\overline{M}_n$ of ~27,700 g/mol (Scheme 1). Nanocomposite solutions were prepared by adding a sonicated suspension of SWNTs in DMAc to a stirred solution of the pre-made oligomer affording mixtures with various weight loadings of SWNT (EA and NAT). Solutions were stirred for ~16 h at ambient temperature prior to film casting. Once dried to a tack free state, the films were cured to 300°C in flowing air to effect imidization and condensation of the silanol groups generated from the alkoxysilane endgroups. An acid catalyst was not required for the hydrolysis and condensation of the alkoxysilane endgroups due to the acidic nature of the amide acid.

To assess dispersion, films amenable to HRSEM were evaluated. The image obtained for the 0.5 wt% NAT-SWNT film showed that the SWNTs were uniformly dispersed throughout the matrix (Figure 3). This was typical for films that could be analyzed by HRSEM due to their conductivity.

In general, the Tg and room temperature thin film tensile properties were unaffected by the low loading levels of SWNTs employed. Similar results have been previously reported (8). The Tg

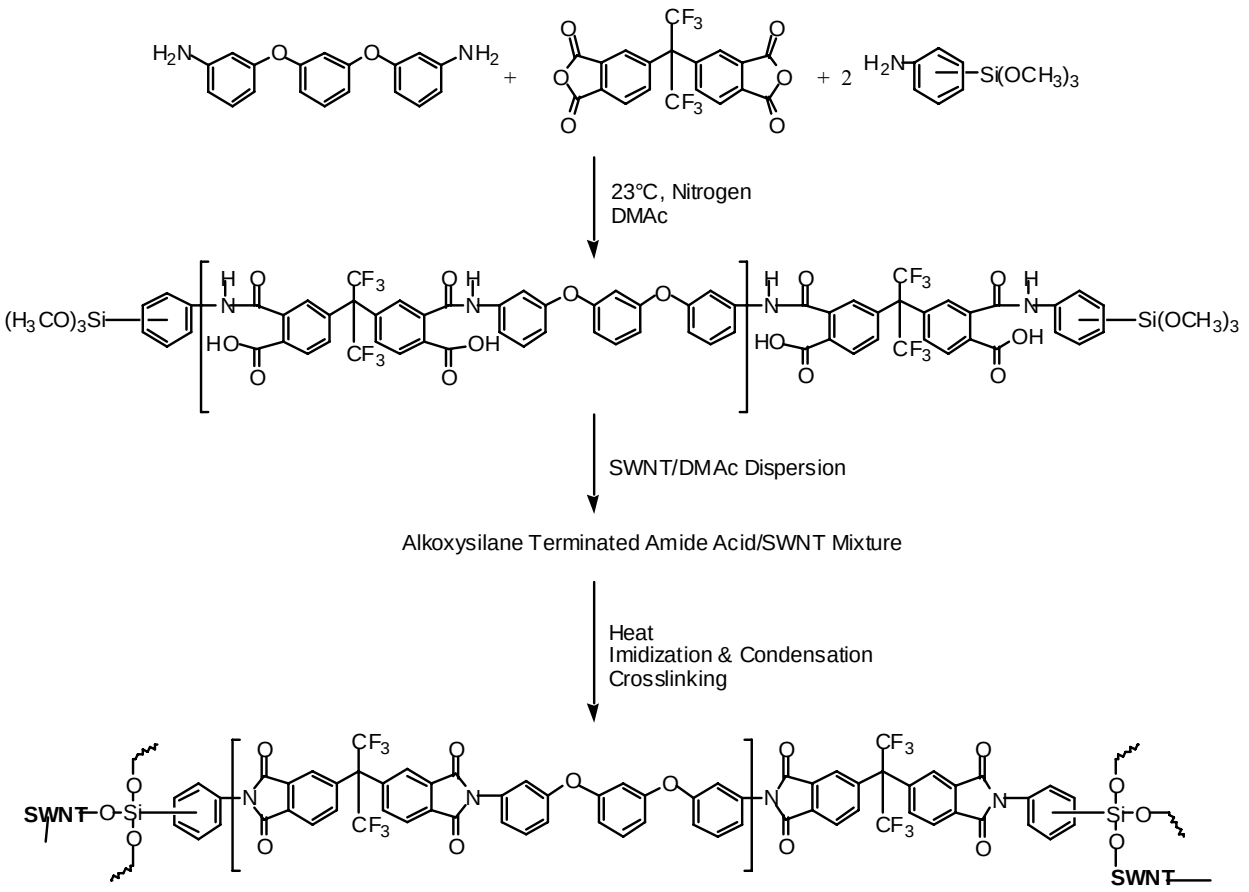

Scheme 1: Synthesis of SWNT nanocomposites from Alkoxysilane Terminated Amide Acids

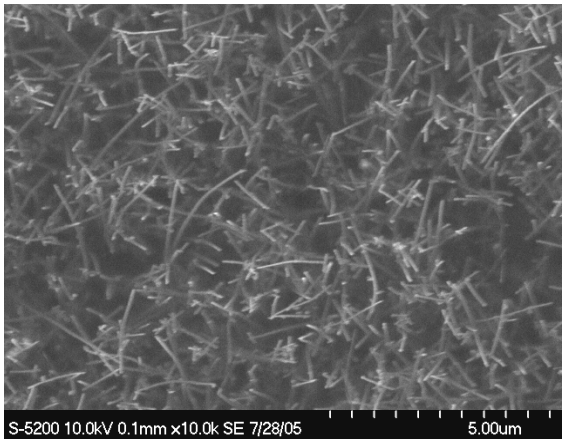

Figure 3. HRSEM image of VI containing 0.5 wt% loading NAT-SWNT.

was ~206°C. The tensile strength, modulus, and elongation at break were ~120 MPa, 3.2 GPa, and 5%, respectively.

The % transmission (%T) at 500 nm (solar maximum), the solar absorptivity (α) and thermal emissivity (ε) of the nanocomposite films are reported in Table 1. These properties are known to be dependent on film thickness and all attempts were made to obtain films of similar thickness. Film thicknesses ranged from 45 to 47.5 μm thus allowing comparisons to be made without normalization. In general, as SWNT loading increased the %T of the films decreased while α and ε increased. Similar results were obtained from HiPco SWNT nanocomposite films (8). A similar trend for %T at 500 nm was observed for nanocomposites prepared from LaRC™ CP2 and NAT-SWNTs by the *in-situ* approach (21). No further comparisons could be made to the materials presented here due to the thinner film size reported for those materials. Film IV exhibited a higher %T and lower α compared to film III as a result of tube shortening. The ε was the same regardless of which type of SWNT was used at the 0.08 wt% loading.

Table 1. Optical and Thermo-optical Properties

ID	SWNT Type	SWNT wt %	Film Thickness, μm	%T @ 500 nm	α	ε
I	None	0	47.5	85	0.06	0.60
II	EA-SWNT	0.05	47.5	65	0.23	0.61
III	EA-SWNT	0.08	47.5	47	0.34	0.61
IV	NAT-SWNT	0.08	45	58	0.27	0.60
V	NAT-SWNT	0.35	47.5	16	0.62	0.69
VI	NAT-SWNT	0.5	47.5	11	0.69	0.71

Electrical conductivity was determined as surface resistance and volume resistivity (Table 2). Similar to nanocomposite films containing HiPco SWNTs (8), the nanocomposite films presented here showed a decrease in the surface resistance with the incorporation of SWNTs (EA and NAT). However, the volume resistivity decreased only at higher loading levels for each of the materials. The resistivity of II and III decreased five orders of magnitude between the 0.05 and 0.08 wt% loading of EA-SWNTs, suggesting that the percolation threshold fell within these bounds. Similar results were obtained with HiPco SWNT based materials, but this occurred between a 0.035 and 0.05 wt% loading. The increased loading needed to attain the percolation threshold using EA-SWNTs may be due to the smaller aspect ratio compared to HiPco SWNTs. The NAT-SWNT containing films (IV-VI) did not show a sharp drop in resistivity, even when the SWNT loading was much higher. LaRC™ CP2/NAT-SWNTs nanocomposites prepared via the *in-situ* approach provided comparable volume resistivity results (21). One reason for this may be related to the decreased length (and aspect ratio) of the NAT-SWNTs compared to EA-SWNTs. Another reason discussed further in 3.3 concerns the reaction of alkoxysilane endgroups with the carboxylic acid functionality of NAT-SWNTs.

Table 2. Thin Film Electrical Characterization

ID	SWNT Type	SWNT wt %	Surface Resistance, Ω/sq	Volume Resistivity, Ω cm
I	None	0	1.4×10^{14}	Not Determined
II	EA-SWNT	0.05	8.1×10^{11}	6.1×10^{14}
III	EA-SWNT	0.08	8.0×10^{6}	2.6×10^{9}
IV	NAT-SWNT	0.08	7.4×10^{11}	6.0×10^{14}
V	NAT-SWNT	0.35	9.8×10^{10}	2.3×10^{12}
VI	NAT-SWNT	0.5	8.2×10^{9}	1.2×10^{11}

3.3 Nanocomposites Prepared from LaRC™ CP2 Amide Acids As seen from Table 2, a higher loading of NAT-SWNTs (IV-VI) was needed to achieve comparable resistivity levels to the EA-SWNTs (II-III). It was initially suggested that this was due to the decreased length of the NAT-SWNTs. Another explanation may be related to the expected chemical bonding between the ASTAA oligomer and NAT-SWNTs. To determine if this was the case, films were prepared from the NAT-SWNTs and imidized LaRC™ CP2 to eliminate the possibility of any chemical reaction between the polymer and the carboxylic acid groups on NAT-SWNTs. The HRSEM image of XII containing 0.35 wt% NAT-SWNTs showed that the SWNTs were uniformly dispersed in the nanocomposite (Figure 4).

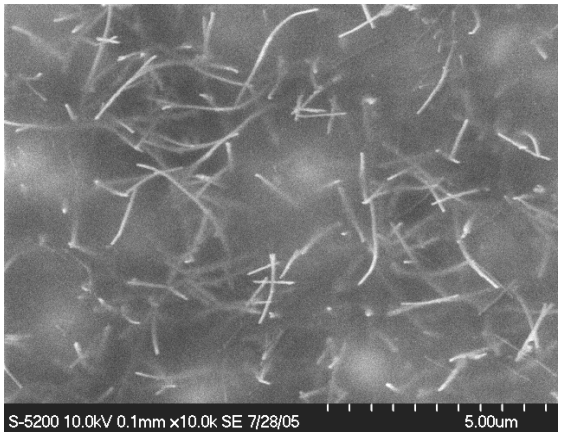

Figure 4. HRSEM image of XII containing 0.35 wt% NAT-SWNT in LaRC™ CP2.

The resistivity data for these nanocomposite films in Table 3 show that the 0.08 wt% loading NAT-SWNTs in LaRC™ CP2 (Film X) exhibited 2-3 orders of magnitude lower resistivity than that obtained for NAT-SWNTs in the ASTAA based material (Table 2, film IV) and for nanocomposites prepared by the *in-situ* approach (21). Additionally, the 0.03 wt% NAT-SWNT/LaRC™ CP2 film exhibited a resistivity 1-2 orders of magnitude lower than the 0.08 wt% ASTAA NAT-SWNT and 0.05 wt% EA-SWNT based materials. This implies that reaction between NAT-SWNTs and the matrix did influence the resistivity of the resultant nanocomposite.

Table 3: Thin Film Electrical Properties

ID	SWNT wt %	Surface Resistance, Ω/sq	Volume Resistivity, Ω cm
VII	0	6.2×10^{11}	4.2×10^{14}
VIII	0.03	4.1×10^{10}	6.9×10^{12}
IX	0.05	8.8×10^{9}	2.9×10^{11}
X	0.08	4.2×10^{9}	8.5×10^{10}
XI	0.1	1.3×10^{9}	2.4×10^{10}
XII	0.35	4.7×10^{7}	1.7×10^{9}

The optical and thermo-optical properties of NAT-SWNTs in LaRC™ CP2 are presented in Table 4. The film thicknesses were similar to those reported in Table 1 so a direct comparison could be made. These properties were essentially the same for base polymer films I and VII and shows that the endgroups had minimal effects. These properties for the 0.08 wt% loading of NAT-SWNTs were comparable regardless of the base polymer.

Table 4. Optical and Thermo-optical Properties

wt %	Thickness, μm	%T @ 500 nm	α	ε
0	45	85	0.07	0.57
0.03	45	71	0.16	0.60
0.05	45	67	0.19	0.60
0.08	45	62	0.24	0.61
0.1	45	56	0.29	0.62
0.35	45	22	0.57	0.68

As observed with the ASTAA based SWNT nanocomposites, the Tg and room temperature thin film tensile properties were unaffected by the NAT-SWNTs loading at these low levels.

4. SUMMARY

Nanocomposite films were prepared from EA- and NAT- SWNTs and functionalized and unfunctionalized LaRC™ CP2 with the SWNTs (EA and NAT) being uniformly dispersed throughout both matrices. The EA-SWNTs based nanocomposites provided similar properties to those prepared from HiPco SWNTs (8). Electrical properties for NAT-SWNTs were found to be matrix dependent due to reaction between the ASTAA oligomer and the nanotubes. Optical and thermo-optical properties of NAT-SWNTs were unaffected by the type of matrix.

The use of trade names or manufacturers does not constitute an official endorsement of such products or manufacturers, either expressed or implied, by the National Aeronautics and Space Administration.

6. REFERENCES

1. C. H. M. Jenkins, Gossamer Spacecraft: Membrane and Inflatable Structures Technology for Space Applications, Vol. 191, American Institute of Aeronautics and Astronautics 2001.
2. RE Smith and GS West, compilers. Space and planetary environment criteria for use in space vehicle development, 1982 Revision. vol. 1.Washington, DC, USA: NASA TM 82478; 1982.
3. AS Jursa, editor. Handbook of geophysic and the space environment, Air Force Geophysics Laboratory, Air Force Systems Command USAF, NTIS Document ADA 167000; 1981.
4. The Radiation Design Handbook, ESA PSS-01-609 (draft). Paris:European Space Agency; 1989.
5. KA Watson, FL Palmieri, and JW Connell, Macromolecules,35, 4968 (2002).
6. SRS Technologies. Huntsville. AL 35806. http://www.stg.srs.com/atd /polyimimidesales /cp_prop.htm
7. C Park, Z Ounaies, KA Watson, RE Crooks,. JG Smith Jr, SE Lowther, JW Connell, EJ Siochi, JS Harrison and TL St. Clair, Chem Phys Lett, 364, 303 (2002).
8. JG Smith Jr., K A Watson, , JW Connell, , DM Delozier, PT Lillehei, Y Lin, B. Zhou, and YP Sun, Polymer, 45, 825-830 (2004).
9. JG Smith Jr., DM Delozier, JW Connell, and KA Watson, Polymer, 45, 6133 (2004).
10. KA Watson, DM Delozier, JG Smith, Jr. and JW Connell. Polymer, 45, 2076 (2005).
11. PJ Glatkowski, P Mack, JL Conroy, JW Piche, P Winsor. US Patent 6,265,466 B1, issued July 24; 2001 to Eikos, Inc.
12. PJ Glatkowski. Sci Adv Mat Proc Eng Proc.,48,2146 (2003).
13. M. Kaempgen, GS Duesberg, and S Roth, Applied Surf. Sci., 252. 425 (2005).
14. N Ferrer-Anglada, M Kaempgen, V Skakalova, U Dettlaf-Weglikowska, and S. Roth, Diamond and Related Matls, 13, 256 (2004).
15. E.T. Thostenson, Z. Ren, and T.W. Chou, Comp. Sci. and Tech., 61, 1899 (2001).
16. J.L. Bahr, E.T. Mickelson, M.J. Bronikowski, R.E. Smalley, J.M. Tour, Chem. Commun., 2001, 193 (2001).
17. H Hu, B Zhao, ME Itkis, and RC Haddon, J. Phys. Chem. B, 107, 13838 (2003).
18. H Hu, A Yu, E Kim, B Zhao, ME Itkis, E Bekyarova, and RC Haddon, J Phys. Chem. B, 109, 11520 (2005).
19. MA Hannon, ME Itkis, S Niyogi, T Alvaraez, C Kuper, M Menon, and RC Haddon, J. Am. Chem. Soc., 123, 11292 (2001).
20. ME Itkis,D Perea, S Niyogi, S Rickard, M Hamon, H Hu, B Zhao, and RC Haddon, Nano Lett., 3, 309 (2003).
21. A Yu, H Hu, E Bekyarova, ME Itkis, J Gao, B Zhao, and RC Haddon, Comp. Sci. and Tech., in press (2005).
22. C Journet, WK Maser, P Bernier, A Loiseau, M Lamy de la Chappelle, S Lefrant, P Deniard, R Lee, and JE Fischer, Nature, 388, 756 (1997).

23. ME Itkis, D Perea, S Niyogi, J Love, J Tang, A Yu, C Kang, R Jung, and RC Haddon, J Phys. Chem. B, 108, 12770 (2004).